Journal of Dynamics and Differential Equations, Vol. 10, No. 2, 1998

Resonant Hopf–Hopf Interactions in Delay Differential Equations

Sue Ann Campbell[1, 2] **and Victor G. LeBlanc**[3]

Received December 15, 1995

A second-order delay differential equation (DDE) which models certain mechanical and neuromechanical regulatory systems is analyzed. We show that there are points in parameter space for which 1:2 resonant Hopf–Hopf interaction occurs at a steady state of the system. Using a singularity theoretic classification scheme [as presented by LeBlanc (1995) and LeBlanc and Langford (1996)], we then give the bifurcation diagrams for periodic solutions in two cases: variation of the delay and variation of the feedback gain near the resonance point. In both cases, period-doubling bifurcations of periodic solutions occur, and it is argued that two tori can bifurcate from these periodic solutions near the period doubling point. These results are then compared to numerical simulations of the DDE.

KEY WORDS: Delay differential equations; resonant double Hopf bifurcation; normal forms.

1. INTRODUCTION

Many biological and physical systems use regulatory feedback mechanisms. Often the communication times in these systems are such that time delays must be incorporated in the feedback loops, leading to models comprising delay differential equations (DDEs). In this paper we consider the second-order DDE

$$\ddot{u} + \alpha\dot{u} + \beta u = f(u(t-\tau)) \tag{1.1}$$

[1] Department of Applied Mathematics, University of Waterloo, Waterloo, Ontario, Canada N2L 3G1.

[2] Center for Nonlinear Dynamics in Physiology and Medicine, McGill University, Montréal, Québec, Canada.

[3] Department of Mathematics and Statistics, University of Ottawa, Ottawa, Ontario, Canada K1N 6N5.

1040-7294/98/0400-0327$15.00/0

where $\tau > 0$, $\beta > 0$, $f: \mathbb{R} \mapsto \mathbb{R}$ is smooth and there exists u^* such that $\beta u^* = f(u^*)$. This equation arises as a paradigm for a number of mechanical or neuromechanical systems in which inertia plays an important role [1, 3, 7] (see also Ref. 5 and references therein).

Milton *et al.* [5, 6, 15, 16] have studied this equation in the context of the pupil light reflex. In this work they showed the existence of points of double Hopf bifurcation and used a center manifold/normal form analysis to predict the behavior of the full equations near such points. They considered only the case when the double Hopf was nonresonant, as little is known about the normal forms for such bifurcations when they are resonant. However, in Ref. 4 it has been shown that double Hopf bifurcations with all resonances of the form $\omega_1 : \omega_2 = (2k+1) : 2l$ for all $k, l \in \mathbb{Z}$, $l \neq 0$ can occur in (1.1). Further, in Ref. 13 the normal forms for the case $\omega_1 : \omega_2 = 1:2$ and all perturbations of this case have been obtained, and the corresponding bifurcation diagrams have been classified. There, it was shown that in a neighborhood of a 1:2 resonant double Hopf point, one can get period-doubling bifurcation of periodic orbits, hysteresis on branches of periodic orbits, and the existence of "noncritical" branches of periodic solutions, i.e., solutions which are local but do not bifurcate from the origin. None of these properties can be captured in a nonresonant Hopf–Hopf analysis. Thus we consider here the case of 1:2 resonant double Hopf bifurcation in (1.1), using the techniques of Refs. 13 and 14.

The outline of the paper is as follows. In Section 2 we establish a set of parameter values for which 1:2 resonant Hopf bifurcation of the equilibrium solution of (1.1) occurs. In Section 3 we perform a center manifold projection and normal form reduction of (1.1), obtaining a set of ordinary differential equations approximating the flow of the full equation near a 1:2 resonant double Hopf bifurcation point. In Section 4 we consider as an example a specific point in parameter space and calculate the expected unfoldings near that point. In Section 5 we consider the linearized stability of the equilibrium solution for parameter values in the neighborhood of the point of Section 4. In Section 6 we show numerical simulations of the full delay differential equation for parameter values in the neighborhood of the point of Section 4 and compare the results with the predictions of the normal form analysis. Finally, in Section 7 we discuss our results.

2. 1:2 RESONANT DOUBLE HOPF POINTS

In this section, we study the stability of the equilibrium solution $u(t) \equiv u^*$ to (1.1). In particular, we establish the existence of parameter values for which the equilibrium solution undergoes two simultaneous Hopf bifurcations with frequencies at a 1-to-2 ratio.

We first eliminate one of the parameters in (1.1). Note that since $\beta > 0$ in (1.1), we can rescale time and relabel u, α, τ, and f so that (1.1) becomes

$$\ddot{u} + \alpha\dot{u} + \tfrac{5}{2}u = f(u(t-\tau)) \tag{2.1}$$

The reason for the choice of the constant $\frac{5}{2}$ for β soon becomes apparent.

The linearization of (2.1) near the equilibrium solution is ($x = u - u^*$),

$$\ddot{x} + \alpha\dot{x} + \tfrac{5}{2}x = Ax(t-\tau) \tag{2.2}$$

where $A \equiv f'(u^*)$ is assumed to be nonzero. We substitute the ansatz $x(t) = e^{\nu t}$ into (2.2), where ν is a complex parameter, to obtain the characteristic equation

$$\nu^2 + \alpha\nu + \tfrac{5}{2} = Ae^{-\nu\tau} \tag{2.3}$$

For given values of α, τ, and A, a necessary condition for Hopf bifurcation to occur at the equilibrium solution of (2.1) is that there exists an $\omega \neq 0$ such that $\nu = i\omega$ is a solution to (2.3). This leads to a pair of real equations

$$\tfrac{5}{2} - \omega^2 = A\cos\omega\tau \tag{2.4a}$$

$$\alpha\omega = -A\sin\omega\tau \tag{2.4b}$$

Note that (2.4a) and (2.4b) are invariant under the reflection $\omega \to -\omega$. Therefore, we assume without loss of generality that $\omega > 0$.

Definition 1. *The point* (α, τ, A) *in parameter space is a* 1:2 resonant double Hopf point *if the following two conditions hold:*

(a) there exists one and only one $\omega > 0$ *such that (2.4a), (2.4b), and*

$$\tfrac{5}{2} - 4\omega^2 = A\cos 2\omega\tau \tag{2.4c}$$

$$2\alpha\omega = -A\sin 2\omega\tau \tag{2.4d}$$

are satisfied, and

(b) if (α, τ, A) *and* ω *are as in (a), then there are no* $\tilde{\omega} \neq \omega, 2\omega$ *such that* $\nu = i\tilde{\omega}$ *satisfies (2.3).*

Proposition 1. *The 1:2 resonant double Hopf points are precisely those in the set*

$$R_{1:2} \equiv \{(\alpha, \tau, A) = (0, (2k+1)\pi, -\tfrac{3}{2}), k = 0, 1, 2,...\}$$

The associated value of ω for these points is 1.[4]

Proof. If $\alpha = 0$, then (2.4b) and (2.4d) imply that $\omega\tau = n\pi$, where n is an integer. Squaring both (2.4a) and (2.4b) and then adding yields

$$A^2 = \tfrac{25}{4} - 5\omega^2 + \omega^4 \tag{2.5}$$

while doing the same with (2.4c) and (2.4d) yields

$$A^2 = \tfrac{25}{4} - 20\omega^2 + 16\omega^4 \tag{2.6}$$

Comparing (2.5) and (2.6) gives

$$\omega^2 = 1 \tag{2.7}$$

which in turn implies that $\tau = n\pi$. Substituting (2.7) into (2.4a) and (2.4c) leads to $A = -\frac{3}{2}$ and $n = 2k+1$, $k = 0, 1, 2,...$.

If $\alpha \neq 0$, it can be shown that one arrives at the contradiction $\omega^2 = -(\alpha^2/9)$. Now suppose that there exists an $\tilde{\omega} \neq 1, 2$ such that

$$\tfrac{5}{2} - \tilde{\omega}^2 = -\tfrac{3}{2}\cos\tilde{\omega}(2k+1)\pi$$

$$\sin\tilde{\omega}(2k+1)\pi = 0$$

i.e., $\nu = i\tilde{\omega}$ satisfies (2.3). This leads to

$$\tilde{\omega} = \frac{\ell}{2k+1}, \qquad \ell \text{ integer}$$

which implies that

$$5 - 2\frac{\ell^2}{(2k+1)^2} = -3(-1)^\ell \Rightarrow \tilde{\omega} = 1 \text{ or } 2$$

which is a contradiction.

Thus, the 1:2 resonant double Hopf points are precisely those given by $R_{1:2}$. □

[4] This is the reason for rescaling β to $\frac{5}{2}$.

3. CENTER MANIFOLD AND NORMAL FORMS

To study the behavior of Eq. (2.1) near the resonant double Hopf point, we need to understand the effects of the nonlinear terms in the equation. To do this we must first reformulate the equation. Rewriting (2.1) as a system of two first-order equations and expanding this around the equilibrium solution ($x_1 = u - u^*$, $x_2 = \dot{u}$) gives

$$\begin{aligned} \dot{x}_1(t) &= x_2(t) \\ \dot{x}_2(t) &= -\tfrac{5}{2}x_1 - \alpha x_2 + Ax_1(t-\tau) + A_2 x_1^2(t-\tau) + O(x_1^3(t-\tau)) \end{aligned} \tag{3.1}$$

Here $A = f'(u^*)$, $A_2 = \frac{1}{2}f''(u^*)$, and we assume that x_1 is small (we are near the equilibrium solution) so that the Taylor expansion of f is valid. Neglecting the higher-order terms, this becomes, in vector form,

$$\dot{\mathbf{x}}(t) = B\mathbf{x}(t) + D\mathbf{x}(t-\tau) + D_2\mathbf{x}(t-\tau)^2 \tag{3.2}$$

where $\mathbf{x} = [x_1, x_2]^T$ and B, D, D_2 are matrices. Let us define the function space $\mathscr{C} \stackrel{\text{def}}{=} C([-\tau, 0], \mathbb{R}^2)$ and the function $\mathbf{x}_t(\theta) = \mathbf{x}(t+\theta)$, $-\tau \leqslant \theta \leqslant 0$. Assuming that $\mathbf{x}_t \in \mathscr{C}$, (3.2) induces an equation on $\mathscr{C}$:

$$\frac{d}{dt}\mathbf{x}_t(\theta) = (\mathscr{L}\mathbf{x}_t)(\theta) + (\mathscr{N}\mathbf{x}_t)(\theta) \tag{3.3}$$

where $\mathscr{L}$ and $\mathscr{N}$ represent operators on $\mathscr{C}$ corresponding to the linear and nonlinear parts of (3.2), respectively. The theory of such functional equations can be found in e.g., Refs. 9 and 11; we review briefly the results needed for our analysis. The linear part of (3.3)

$$\frac{d}{dt}\mathbf{x}_t(\theta) = (\mathscr{L}\mathbf{x}_t)(\theta) \tag{3.4}$$

has the same spectrum as the linearization of the original Eq. (2.2). Therefore when the parameters lie in the set $R_{1:2}$ of Proposition 1, (3.4) has two pairs of pure imaginary eigenvalues, $\pm i$, $\pm 2i$, and no other eigenvalues on the imaginary axis. We assume (see Section 5) that the noncritical eigenvalues have negative real parts. In this situation there exists a splitting of the phase space $\mathscr{C} = \mathscr{P} \oplus \mathscr{Q}$, where $\mathscr{P}$ is a four-dimensional subspace spanned by the solutions of (3.4) corresponding to the pure imaginary eigenvalues, $\mathscr{Q}$ is infinite dimensional and both $\mathscr{P}$ and $\mathscr{Q}$ are invariant

under the flow associated with (3.4). For the nonlinear equation, some of this structure is retained: $\mathscr{C}$ now contains a four-dimensional invariant (center) manifold, the flow on which is a good approximation for the long-term behavior of solutions to the full nonlinear equation. This flow is determined by the basis for $\mathscr{P}$ and a four-dimensional vector $\mathbf{z}(t) = [z_1(t), z_2(t), z_3(t), z_4(t)]^T$ which satisfies the following set of four first-order ordinary differential equations:

$$\dot{z}_1 = -z_2 + f^1_{11} z_1^2 + f^1_{12} z_1 z_2 + f^1_{13} z_1 z_3 + \cdots + f^1_{44} z_4^2 + O(3) \tag{3.5a}$$

$$\dot{z}_2 = z_1 + f^2_{11} z_1^2 + f^2_{12} z_1 z_2 + f^2_{13} z_1 z_3 + \cdots + f^2_{44} z_4^2 + O(3) \tag{3.5b}$$

$$\dot{z}_3 = -2z_4 + f^3_{11} z_1^2 + f^3_{12} z_1 z_2 + f^3_{13} z_1 z_3 + \cdots + f^3_{44} z_4^2 + O(3) \tag{3.5c}$$

$$\dot{z}_4 = 2z_3 + f^4_{11} z_1^2 + f^4_{12} z_1 z_2 + f^4_{13} z_1 z_3 + \cdots + f^4_{44} z_4^2 + O(3) \tag{3.5d}$$

Here the f^k_{ij} are functions of the original model parameters τ, A, A_2, for example,

$$f^1_{12} = -\frac{4\sqrt{2}\, A_2 \sqrt{\sqrt{A^2\tau^2+4} - A\tau}}{(A^2\tau^2+4)^{3/2}} \tag{3.6}$$

See, e.g., Refs. 5 and 18 for more details on how this calculation is performed. We have thus reduced our second-order delay differential equation to a system of four ordinary differential equations. The linearization of this system at the origin has two pairs of pure imaginary eigenvalues in 1:2 resonance and thus a nonlinear change of coordinates puts the system into the following normal form [13]:

$$\dot{v}_1 = -v_2 + b_1(v_1 v_3 + v_2 v_4) - b_2(v_1 v_4 - v_2 v_3) + O(3) \tag{3.7a}$$

$$\dot{v}_2 = v_1 + b_1(v_1 v_4 - v_2 v_3) + b_2(v_1 v_3 + v_2 v_4) + O(3) \tag{3.7b}$$

$$\dot{v}_3 = -2v_4 + d_1(v_1^2 - v_2^2) - 2d_2 v_1 v_2 + O(3) \tag{3.7c}$$

$$\dot{v}_4 = 2v_3 + 2d_1 v_1 v_2 + d_2(v_1^2 - v_2^2) + O(3) \tag{3.7d}$$

The dependence of the coefficients b_j, d_j on the original parameters of our model can be computed, for example,

$$b_1 = -\frac{|(5/2) - A|^{3/4} \sqrt{2}\, A_2 \sqrt{\sqrt{A^2\pi^2 + 16((5/2)+A)^2} + A\pi}}{\sqrt{A^2\pi^2 + 4((5/2)+A)^2}\, \sqrt{A^2\pi^2 + 16((5/2)+A)^2}} \tag{3.8}$$

Note that, in contrast to standard Hopf bifurcation, we need only to consider terms up to and including quadratic order in Eqs. (3.7a)–(3.7d). This follows from the general classification theory presented by LeBlanc [13] and LeBlanc and Langford [14].

The problem of local bifurcation of periodic solutions of the dynamical system (3.7a)–(3.7d) was studied by LeBlanc [13] and LeBlanc and Langford [14], using techniques from singularity theory. There, all perfect and imperfect bifurcation diagrams were classified, under some generic conditions. As mentioned above, the classification of bifurcation diagrams depends not only on the quadratic coefficients shown above, but also on the linear coefficients and their dependence on the parameters of the original model. In all, there are more than 35 possible unfoldings. We therefore concentrate on one particular double Hopf point and make the specific calculations necessary to compute the unfoldings of the normal form (3.7a)–(3.7d) near this point. This is the subject of the next section.

4. BIFURCATION DIAGRAMS FOR $(0, \pi, -\frac{3}{2}) \in R_{1:2}$

For a physical system which is modeled by (2.1), one is usually interested in the effects of variation of either the delay, τ, or the gain, $A \equiv f'(u^*)$, on the system. This is precisely the framework in which the 1:2 resonance is studied in Refs. 13 and 14, where it is assumed that one of the auxiliary parameters of the differential equations is distinguished. That is, they considered bifurcation diagrams only with respect to variation of this one parameter, while keeping all other parameters fixed. In this section, we give the bifurcation diagrams for periodic solutions associated with both the following cases: either τ or A is distinguished. Our analysis is performed near the point $(\alpha = 0,\ \tau = \pi,\ A = -\frac{3}{2}) \in R_{1:2}$. For both cases, we assume that α is held fixed at 0 and A_2 [see (3.1)] is fixed at 9/10 for definiteness.[5] In the first case, we then assume that A is fixed at A^* near $-\frac{3}{2}$ and that τ varies near π. In the second case, we assume that τ is fixed at τ^* near π and that A varies near $-\frac{3}{2}$. The numerical experiments which are discussed in Section 6 follow the same approach, i.e., vary τ or A while keeping other parameters fixed.

In order to compute the normal forms associated with each of these cases, we need to determine the leading order dependence of the two solutions $\nu_{1,2}(\alpha, \tau, A)$ of (2.3) near $(0, \pi, -\frac{3}{2})$. Since, for our purposes, we are keeping α fixed, we can write

$$\nu_1(0, \tau, A) = i + (m_{11} + i m_{12})(\tau - \pi) + (n_{11} + i n_{12})(A + \tfrac{3}{2}) + \cdots \qquad (4.1)$$

[5] Note that this is not a severe restriction. Indeed, the perturbed bifurcation diagrams that we will obtain must persist under contact equivalence diffeomorphism when (α, A_2) is in some neighborhood of $(0, 9/10)$, since all singularities in these diagrams are codimension 0 (see Refs. 10 and 13).

and

$$v_2(0, \tau, A) = 2i + (m_{21} + im_{22})(\tau - \pi) + (n_{21} + in_{22})(A + \tfrac{3}{2}) + \cdots \tag{4.2}$$

where the real quantities m_{ij} and n_{ij} are obtained from implicit differentiation of (2.3) and are equal to

$$\begin{aligned} m_{11} &= -\frac{12}{9\pi^2 + 16}, & m_{12} &= -\frac{9\pi}{9\pi^2 + 16}, \\ m_{21} &= \frac{48}{9\pi^2 + 64}, & m_{22} &= -\frac{18\pi}{9\pi^2 + 64} \end{aligned} \tag{4.3}$$

and

$$\begin{aligned} n_{11} &= -\frac{6\pi}{9\pi^2 + 16}, & n_{12} &= \frac{8}{9\pi^2 + 16}, \\ n_{21} &= -\frac{6\pi}{9\pi^2 + 64}, & n_{22} &= -\frac{16}{9\pi^2 + 64} \end{aligned} \tag{4.4}$$

Also needed for the classification of the normal forms are the nonlinear coefficients b_1, b_2, d_1, and d_2 of the resonant vector field (3.7a)–(3.7d). The exact values are given by complicated expressions similar to (3.8). we give here only the first few significant digits of the decimal expansions of these coefficients:

$$b_1 \approx -0.04875, \qquad b_2 \approx 0.13276 \tag{4.5a}$$

$$d_1 \approx -0.00350, \qquad d_2 \approx -0.07063 \tag{4.5b}$$

4.1. Distinguished Parameter: τ

In this case, we supposed that $A = A^*$ near $-\frac{3}{2}$, and let $\tilde{\lambda} = \tau - \pi$ be the distinguished bifurcation parameter and $\varepsilon = A^* + \frac{3}{2}$ be an unfolding parameter. This then leads to the following unfolding of (3.7a)–(3.7d):

$$\begin{aligned} \dot{v}_1 = {} & (m_{11}\tilde{\lambda} + n_{11}\varepsilon)\, v_1 - (1 + m_{12}\tilde{\lambda} + n_{12}\varepsilon)\, v_2 + \tilde{b}_1(v_1 v_3 + v_2 v_4) \\ & - \tilde{b}_2(v_1 v_4 - v_2 v_3) + O(3) \end{aligned} \tag{4.6a}$$

$$\begin{aligned} \dot{v}_2 = {} & (1 + m_{12}\tilde{\lambda} + n_{12}\varepsilon)\, v_1 + (m_{11}\tilde{\lambda} + n_{11}\varepsilon)\, v_2 + \tilde{b}_1(v_1 v_4 - v_2 v_3) \\ & + \tilde{b}_2(v_1 v_3 + v_2 v_1) + O(3) \end{aligned} \tag{4.6b}$$

$$\dot{v}_3 = (m_{21}\tilde{\lambda} + n_{21}\varepsilon)\, v_3 - (2 + m_{22}\tilde{\lambda} + n_{22}\varepsilon)\, v_4 + \tilde{d}_1(v_1^2 - v_2^2) - 2\tilde{d}_2 v_1 v_2 + O(3) \tag{4.6c}$$

$$\dot{v}_4 = (2 + m_{22}\tilde{\lambda} + n_{22}\varepsilon)\, v_3 + (m_{21}\tilde{\lambda} + n_{21}\varepsilon)\, v_4 + 2\tilde{d}_1 v_1 v_2 + \tilde{d}_2(v_1^2 - v_2^2) + O(3) \tag{4.6d}$$

where the m_{ij} and n_{ij} are as in (4.3) and (4.4), and $\tilde{b}_1$, $\tilde{b}_2$, $\tilde{d}_1$, and $\tilde{d}_2$ are near the values given in (4.5a) and (4.5b) when $\tilde{\lambda}$ and ε are small.

In order to be consistent with the notation of Refs. 13 and 14, we let $\lambda \overset{\text{def}}{=} \tilde{\lambda} + (n_{11}/m_{11})\,\varepsilon$. Performing a Liapunov–Schmidt reduction (see, e.g., Chapter VII of Ref. 10) and using the singularity theory developed in Refs. 13 and 14, one can show that bifurcating periodic solutions of (4.6a)–(4.6d) with fundamental period near 2π are in one-to-one correspondence with the zeros of the following system of algebraic equations:

$$\lambda + U = 0 \tag{4.7a}$$

$$(\sigma_1\lambda + \mu)\, U + (\sigma_2\lambda - \eta)\, V + V^2 + aW^2 = 0 \tag{4.7b}$$

$$-(\sigma_2\lambda - \eta)\, U + (\sigma_1\lambda + \mu)\, V - UV + \delta W^2 = 0 \tag{4.7c}$$

where

$$\sigma_1 = \frac{m_{21}}{2m_{11}}, \qquad \sigma_2 = \frac{2m_{12} - m_{22}}{2m_{11}} \tag{4.8}$$

$$a = \frac{b_1 d_1 - b_2 d_2}{|b_1 d_2 + b_2 d_1|}, \qquad \delta = \operatorname{sgn}(b_1 d_2 + b_2 d_1) \tag{4.9}$$

$$\mu = \left(\frac{m_{11}n_{21} - m_{21}n_{11}}{2m_{11}^2}\right)\varepsilon,$$
$$\eta = -\left(\frac{2m_{11}n_{12} - 2m_{12}n_{11} + m_{22}n_{11} - m_{11}n_{22}}{2m_{11}^2}\right)\varepsilon \tag{4.10}$$

and $\sqrt{U^2 + V^2 + W^2}$ is approximately the amplitude of the corresponding periodic solution.

When $\varepsilon = 0$, varying λ through 0 causes the critical eigenvalues of (4.6a)–(4.6d) to cross the imaginary axis simultaneously (at $\lambda = 0$) at an exact 1:2 ratio. This is a so-called *perfect bifurcation*. To determine what the associated perfect bifurcation diagram resembles, we again resort to Refs. 13 and 14, where it is necessary to compute the signs of the following quantities:

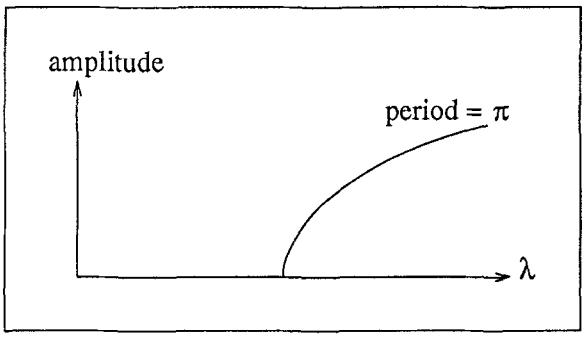

Fig. 1. Perfect bifurcation diagram for variation of τ.

$$\Sigma \stackrel{\text{def}}{=} \sigma_2^2 - 2a\delta\sigma_1\sigma_2 + 2a\delta\sigma_2 + a^2(\sigma_1+1)^2 + 4\sigma_1 \approx 7.73178 > 0 \quad (4.11a)$$

$$\sigma_1 = -2\frac{9\pi^2+16}{9\pi^2+64} < 0 \quad (4.11b)$$

$$a(\sigma_1+1)^2 + \delta\sigma_2(1-\sigma_1) \approx 2.19838 > 0 \quad (4.11c)$$

We conclude that the perfect bifurcation is of type IIa according to the classification scheme of Refs. 13 and 14, and the associated perfect bifurcation diagram is given in Fig. 1. Notice that there are no periodic orbits corresponding to the i mode (fundamental period $=2\pi$) in this bifurcation diagram. This is in contrast to the nonresonant Hopf–Hopf interaction whose perfect bifurcation diagram has two branches of periodic solutions (one for each mode). An example of this is shown in Fig. 2 (see Ref. 12).

When ε is small but nonzero, the critical eigenvalues of (4.6a)–(4.6d) will cross the imaginary axis at distinct values of λ, and the ratio of the

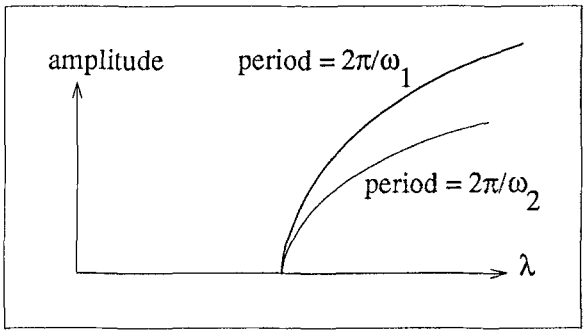

Fig. 2. Perfect bifurcation diagram for $\omega_1:\omega_2$ nonresonant Hopf–Hopf interaction.

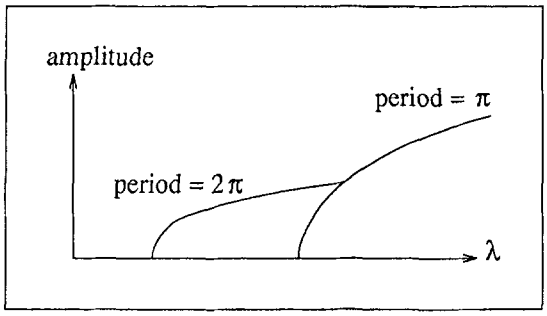

Fig. 3. Perturbation of Fig. 1, $\varepsilon > 0$.

crossing points will be near but not equal to 1:2. We say that the resonance has been split and detuned, with splitting and detuning being given, respectively, by μ and η as in (4.10). The bifurcation diagram will be a perturbation of the one given in Fig. 1. In Refs. 13 and 14, it is shown that there are nine such possible perturbations, up to some equivalence relation. To determine which apply in this case, we observe that

$$-a < \frac{\eta}{\mu} < -\frac{(\sigma_2 + a\delta)}{\sigma_1} \tag{4.12}$$

The perturbed bifurcation diagram will thus be diffeomorphic to that in Fig. 3 if $\varepsilon > 0$ and that in Fig. 4 if $\varepsilon < 0$.

Here we see the appearance of a branch of periodic solutions with fundamental period near 2π which bifurcates from the origin and then disappears in a period-doubling bifurcation on the π-periodic branch. This period-doubling bifurcation is a direct consequence of the proximity to the 1:2 resonance, and one would not be able to predict it using an analysis

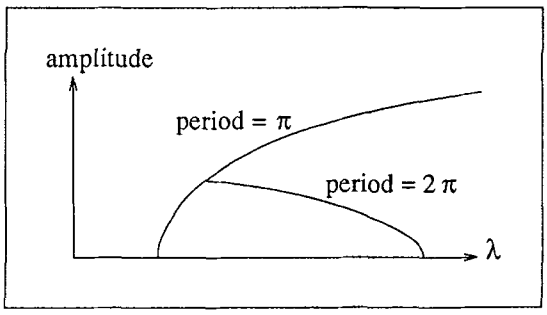

Fig. 4. Perturbation of Fig. 1, $\varepsilon < 0$.

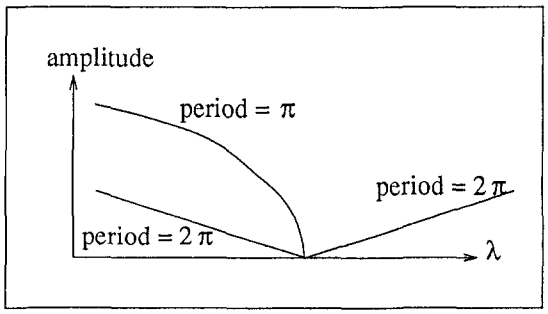

Fig. 5. Perfect bifurcation diagram for variation of A.

such as in Refs. 5 and 6. The asymptotic stability of these periodic solution branches was not determined in Refs. 13 or 14. However, it was shown in Ref. 13 that this particular period-doubling bifurcation is related to the problem of loss of stability of self-sustained oscillations studied by Arnold [2] and Takens [17] and leads to possible secondary bifurcation of two-frequency tori from both the π branch and the 2π branch near the point of period-doubling. We discuss stability in Section 5 and the tori in Section 6.

We also remark that for λ and ε small enough, the classification conditions (4.11a), (4.11b), and (4.11c) will remain valid when b_1, b_2, d_1, and d_2 are replaced by $\tilde{b}_1$, $\tilde{b}_2$, $\tilde{d}_1$, and $\tilde{d}_2$ [see (4.6a)-(4.6d)].

4.2. Distinguished Parameter: A

We now reverse the roles of τ and A, i.e., we set $\tau = \tau^*$ near π, and let $\tilde{\lambda} = A + \frac{3}{2}$ and $\varepsilon = \tau^* - \pi$. The effect of this is that σ_1, σ_2, μ, and η are defined by the same formulas as (4.8) and (4.10), but with the m_{ij} and the n_{ij} interchanged. Thus, Σ [as defined by (4.11a)] is now $\approx 17.3978 > 0$, and

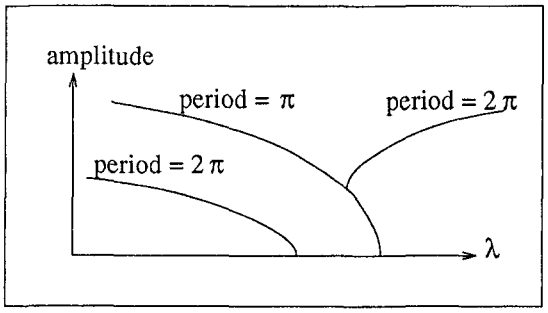

Fig. 6. Perturbation of Fig. 5, $\varepsilon > 0$.

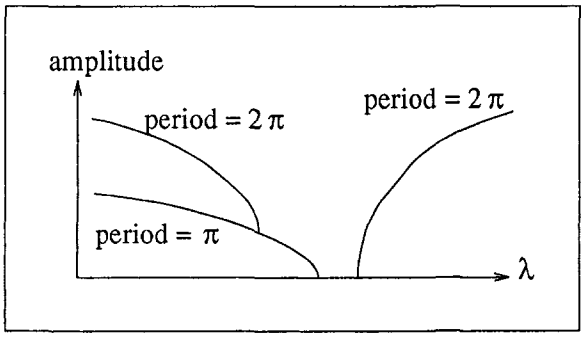

Fig. 7. Perturbation of Fig. 5, $\varepsilon < 0$.

$\sigma_1 \approx 0.3430 > 0$. It follows that the perfect bifurcation diagram for variation of A is of type IIb, according to the classification scheme of Refs. 13 and 14, and is shown in Fig. 5. Note the difference between Fig. 5 and Fig. 2.

There are 11 possible unfoldings in this case. For η and μ as given here, a straightforward computation shows that the unfoldings which apply are as in Fig. 6 if $\varepsilon > 0$ and Fig. 7 if $\varepsilon < 0$.

The relationships between these various figures is clarified by considering the (A, τ)-plane, as shown in Fig. 8. Each of the diagrams in Figs. 1 and 3–7 may be seen as a path in the (A, τ)-plane in a neighborhood of the point $(-\frac{3}{2}, \pi)$. Paths 1 and 5 pass exactly through this point of 1:2 resonance (perfect bifurcations), whereas the other paths generate unfoldings (perturbations) of these perfect bifurcation diagrams. Apart from the period-doubling bifurcations, one of the striking features of the 1:2 resonance is that the direction of bifurcation of the primary 2π branch changes along the 2π bifurcation curve from one side to the other of the primary π bifurcation curve. This is not the case in nonresonant Hopf–Hopf interaction. The reason for this is that the leading order nonlinearities in the resonant problem are quadratic, whereas they are cubic in the nonresonant interaction.

5. STABILITY ANALYSIS

In order to compare our analysis of Section 4 to numerical simulations of the full delay differential equation, it is useful to consider the linearized stability of the equilibrium solution to Eq. (1.1). This will allow us to conjecture which of the limit cycles predicted by the analysis of Section 4 will be stable and hence observable by numerical simulations.

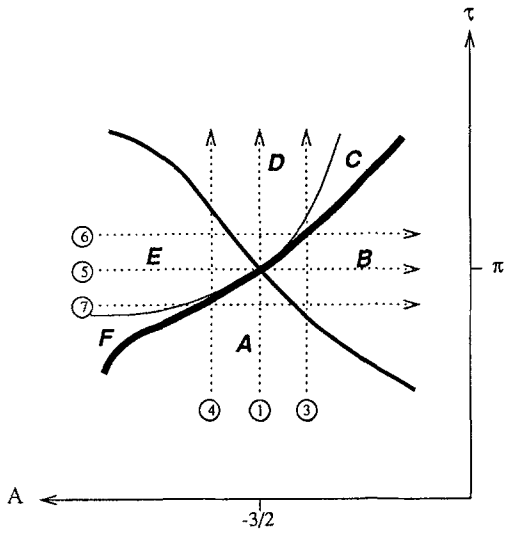

Legend:

primary Hopf bifurcation curve: period = π

primary Hopf bifurcation curve: period = 2π

period-doubling bifurcation curve

A no periodic solutions
B one 2π -periodic solution, no π -periodic solution
C one 2π -periodic solution, one π -periodic solution
D one π -periodic solution, no 2π-periodic solution
E one 2π -periodic solution, one π -periodic solution
F one π -periodic solution, no 2π-periodic solution

Ⓝ : bifurcation diagram of figure N

Fig. 8. Figures 1 and 3–7 as paths in the (A, τ)-plane.

In the case of no damping ($\alpha = 0$), the linearization (2.2) of the nonlinear delay differential equation about the equilibrium solution becomes

$$\ddot{x} + \tfrac{5}{2}x = Ax(t-\tau) \tag{5.1}$$

The corresponding characteristic equation is

$$v^2 + \tfrac{5}{2} = Ae^{-v\tau} \tag{5.2}$$

When $A=0$, i.e., along the τ axis, we have $\nu=\pm i\sqrt{5/2}$. This is just the usual result of neutral stability for the simple harmonic oscillator with no forcing. Now, putting $\alpha=0$ in Eqs. (2.4b) and (2.4d) we have $\omega\tau=\pi$, and the two priory Hopf bifurcation curves are given by

$$A=\omega^2-\frac{5}{2}=\frac{\pi^2}{\tau^2}-\frac{5}{2} \qquad (2\pi \text{ bifurcation curve}) \tag{5.3a}$$

$$A=\frac{5}{2}-4\omega^2=\frac{5}{2}-\frac{4\pi^2}{\tau^2} \qquad (\pi \text{ bifurcation curve}) \tag{5.3b}$$

This leads to the following result.

Theorem 1. *The equilibrium solution is linearly stable in the region with $A<0$ enclosed by the two Hopf bifurcation curves (5.3a)–(5.3b) and the τ axis.*

Proof. We begin by noting that the only way a root of Eq. (5.2) can acquire positive real part is by passing through the imaginary axis, i.e., no root can "come in from positive infinity" (see, e.g., Ref. 8). From (5.2), we have

$$\frac{d\nu}{dA}=\frac{1}{2\nu e^{\nu\tau}+A\tau} \tag{5.4}$$

thus along the τ axis

$$\frac{d}{dA}[\mathrm{Re}(\nu)]\bigg|_{A=0}=-\frac{\sin(\sqrt{5/2}\,\tau)}{\sqrt{10}} \tag{5.5}$$

Now the Hopf curves intersect the τ axis at $\tau=\sqrt{2/5}\,\pi, 2\sqrt{2/5}\,\pi$, respectively, so it is easy to see from (5.5) that

$$\frac{d}{dA}[\mathrm{Re}(\nu)]\bigg|_{A=0}>0 \tag{5.6}$$

between these two points. Thus as A decreases, the real parts of all eigenvalues, $\mathrm{Re}[\nu]$, will also decrease. Since $\mathrm{Re}[\nu]=0$ along $A=0$, we conclude that $\mathrm{Re}[\nu]<0$ for $A<0$, but close to zero. Since no eigenvalue crosses the imaginary axis between $A=0$ and the curves described by Eqs. (5.3a)–(5.3b), all eigenvalues must have negative real parts in this region. □

This region of stability of the equilibrium solution corresponds to region B in Fig. 8. This is consistent with the analysis of Section 4, which

tells us that the real parts of a pair of complex conjugate eigenvalues are decreasing as τ increases across the 2π bifurcation curve ($m_{11} < 0$) and those of another pair are increasing as τ increases across the π bifurcation curve ($m_{21} > 0$). This, together with the criticality of the bifurcations as shown in Figs. 3, 4, 6, and 7, allows us to conjecture that the only stable periodic solutions in Fig. 8 are the π-periodic solutions in region C (at least for some small interval around the primary bifurcation point). We note that Theorem 1 confirms that at the double Hopf bifurcation point, all other eigenvalues have negative real parts, so the center manifold construction of Section 3 is valid.

6. NUMERICAL SIMULATIONS

Numerical simulations were performed using a fourth-order Runge Kutta scheme adapted for delay differential equations, on the following nonlinear equation:

$$\ddot{x} + \tfrac{5}{2}x = Ax(t-\tau) + 0.9x^2(t-\tau) \tag{6.1}$$

Parameter values for A and τ were chosen on the grid shown in Fig. 9. Two sets of constant initial data were used: $x(t) = x_0$, $-\tau \leqslant t \leqslant 0$ with $x_0 = 0.1$ and 0.2. The results are as reported in Table I.

Using parameter values corresponding to regions A, E, and F in Fig. 8, we see either solutions on a two torus, or solutions which increase

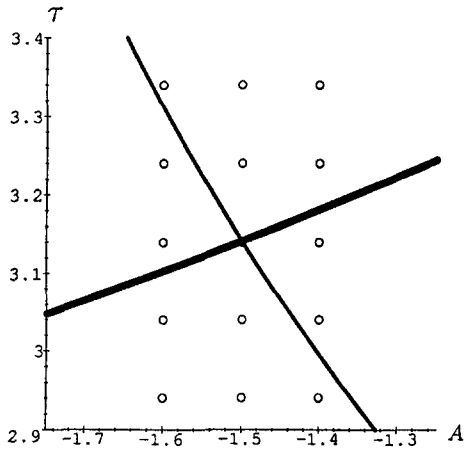

Fig. 9. Bifurcation set showing parameter values for numerical simulations.

Table I. Results of the Numerical Simulation of Eq. (6.1)

	A		
	-1.6	-1.5	-1.4
$\tau\backslash x_0$	0.1\0.2	0.1\0.2	0.1\0.2
3.34	Unbounded	Unbounded	Torus
3.24	Unbounded	Unbounded	Torus
3.14	Unbounded	Torus	Equilibrium\torus
3.04	Unbounded	Torus	Equilibrium\torus
2.94	Unbounded	Torus	Torus

without bound. This is consistent with the conjecture that none of the periodic solutions is stable in these regions.

Using parameter values corresponding to region B in Fig. 8, we see the equilibrium solution for the initial condition $x_0 = 0.1$ and the two-torus solution for the initial condition $x_0 = 0.2$. Note that these tori do not appear directly as solutions of the algebraic Eqs. (4.7a)–(4.7c) since these equations correspond only to periodic solutions of (2.1). However, the period-doubling bifurcation does follow from these algebraic equations (see Refs. 13 and 14). Moreover, as was shown in Ref. 13, this period-doubling is the codimension 2 case studied by Takens [17] and Arnold [2], for which it is known that tori bifurcate from the periodic solutions. We therefore conjecture that the tori which are observed in our numerical simulations are those predicted by the unfolding of the period-doubling bifurcation and are, thus, a local consequence of the 1:2 resonance in (2.1).

It is difficult to determine which parameter values will lie in region C and which in region D in Fig. 8, as we have no expression for the curve of period doubling bifurcation in the coordinates of our delay differential equation. For the parameter values considered, and others taken closer to the π bifurcation curve, we see no evidence of the π-periodic solution. This could be because region C is too thin[6] for us to resolve with our simulations or due to some other bifurcation (e.g., a subcritical bifurcation to a two torus) which renders the π-periodic solutions unstable. In performing other simulations further from the bifurcation point (e.g., at $A = -1$), we do see an almost π-periodic solution, but it exists only in a small range,

[6] It is shown in Ref. 13 that this curve has quadratic tangency to the primary π bifurcation curve at the 1:2 resonant point.

and we are reluctant to relate this to our analysis, as it occurs quite far from the double bifurcation point.

7. DISCUSSION

We have shown that the delay differential equation describing the simple harmonic oscillator with delayed, position-dependent forcing has a countable number of points of 1:2 resonant double Hopf bifurcation. Using center manifold analysis and normal forms, we have reduced the delay differential equation to a set of four ordinary differential equations representing the long-term behavior of the system near the bifurcation point. As might be expected, the normal form predicts the creation of two periodic solutions from the Hopf bifurcations when we are near, but not at resonance. We show that the proximity to the 1:2 resonance causes these periodic solutions to interact through a period doubling bifurcation. The latter bifurcation is related to the problem of stability of self-sustained oscillations studied by Arnold [2] and Takens [17], who showed that two tori may bifurcate from the periodic solutions. Numerical simulations performed on the full nonlinear delay differential equation confirm our analysis and the presence of these two tori.

Our goal here was not to give an exhaustive analysis of the 1:2 resonance in (1.1), but merely to illustrate the occurrence of features which are special to the 1:2 resonance *and which could not be captured by the standard techniques of nonresonant analysis.* It is quite reasonable to expect that by varying other parameters, for example, A_2 (which we have fixed at 9/10 here), one could get bifurcation diagrams where branches of periodic solutions undergo hysteresis, or where branches of periodic solutions exist but do not bifurcate from the origin. Both of these phenomena have been shown to occur in unfoldings of the 1:2 resonance (see Refs. 13 and 14) and are not predicted by the theory of nonresonant Hopf–Hopf interactions.

A variety of mechanical and neuromechanical control systems may be modeled by the harmonic oscillator with delayed, position-dependent feedback. For physical reasons, these systems are generally assumed to have nonzero damping, which precludes the existence of 1:2 resonant double Hopf bifurcation points. It would therefore appear that the results of this paper cannot be applied to these cases of nonzero damping, however, our results hold for any parameter values which are close to those where a 1:2 resonant Hopf bifurcation occurs. In particular, for values of the damping constant close to zero, the behavior discussed above will persist. An illustration of this is the work of Campbell *et al.* [6]. They numerically observed isolated period doubling bifurcations in Eq. (1.1) with small

nonzero damping ($\alpha \approx .07$), for parameter values near a double Hopf bifurcation with frequencies at the ratio $w_1 : w_2 = 0.609 : 1.274$.

ACKNOWLEDGEMENTS

V.G.L. is grateful to the Department of Applied Mathematics of the University of Waterloo, where most of this work was done, and acknowledges financial support from the Natural Sciences and Engineering Research Council of Canada in the form of a 1967 Science and Engineering scholarship and a Postdoctoral Research Fellowship. S.A.C. acknowledges support from the University of Waterloo in the form of a Presidential Starter Grant and the Natural Sciences and Engineering Research Council in the form of an Individual Research Grant.

REFERENCES

1. an der Heiden, U. (1979). Delays in physiological systems. *J. Math. Biol.* **8**, 345–364.
2. Arnold, V. I. (1983). *Geometrical Methods in the Theory of Ordinary Differential Equations*, Springer-Verlag, New York.
3. Boe, E., and Chang, H.-C. (1989). Dynamics of delayed systems under feedback control. *Chem. Eng. Sci.* **44**, 1281–1294.
4. Campbell, S., and Bélair, J. (1995). Resonant codimension two bifurcation in the harmonic oscillator with delayed forcing. Preprint.
5. Campbell, S., Bélair, J., Ohira, T., and Milton, J. (1995). Limit cycles, tori, and complex dynamics in a second-order differential equations with delayed negative feedback. *J. Dynam. Diff. Eq.* **7**, 213–236.
6. Campbell, S., Bélair, J., Ohira, T., and Milton, J. (1995). Complex dynamics and multistability in a damped harmonic oscillator with delayed negative feedback. *Chaos* **5**(4), 640–645.
7. Chung, L., Reinhorn, A., and Soong, T. (1988). Experiments on active control of seismic structures. *J. Eng. Mech.* **114**, 241–256.
8. Cooke, K. L., and Grossman, A. (1982). Discrete delay, distributed delay and stability switches. *J. Math. Anal. Appl.* **86**, 592–627.
9. Diekmann, O., van Gils, S., Lunel, S. V., and Walther, H.-O. (1995). *Delay Equations*, Springer-Verlag, New York.
10. Golubitsky, M., and Schaeffer, D. G. (1985). *Singularities and Groups in Bifurcation Theory, Vol. 1*, Springer-Verlag, New York.
11. Hale, J., and Lunel, S. V. (1993). *Introduction to Functional Differential Equations*, Springer Verlag, New York.
12. Langford, W. F., and Iooss, G. (1980). Interactions of the Hopf and pitchfork bifurcations. In *Bifurcation Problems and Their Numerical Solutions* (International Series on Numerical Mathematics 54), pp. 103–134.
13. LeBlanc, V. (1995). *On the* 1:2 *Resonant Hopf Bifurcation*, Ph.D. thesis, University of Waterloo, Waterloo.
14. LeBlanc, V., and Langford, W. (1996). Classification and unfoldings of 1:2 resonant Hopf bifurcation. *Arch. Ration. Mech. Anal.* **136**, 305–357.

15. Milton, J., and Longtin, A. (1990). Evaluation of pupil constriction and dilation from cycling measurements. *Vision Res.* **30**, 515–525.
16. Milton, J., and Ohira, T. (1993). Dynamics of neuromuscular control with delayed displacement-dependent feedback. In *Differential-Delay Equations and Applications to Biology and Medicine* (World Congress of Nonlinear Analysts).
17. Takens, F. (1973). *Applications of Global Analysis I*, Communications of the Mathematical Institute, Rijksuniversiteit Utrecht, Utrecht.
18. Wischert, W., Wunderlin, A., Pelster, A., Olivier, M., and Groslambert, J. (1994). Delay-induced instabilities in nonlinear feedback systems. *Phys. Rev. E* **49**, 203–219.

Printed in Belgium